Pergamon

Int. J. Heat Mass Transfer. Vol. 38, No. 17, pp. 3313–3317, 1995

0017-9310/95 $9.50+0.00

0017-9310(95)00063-1

TECHNICAL NOTE

2-D numerical study on a rectangular thermosyphon with vertical or horizontal heat transfer sections

YINXUE SU and ZHONGQI CHEN†

Department of Power Machinery Engineering, Xi'an Jiaotong University, Xi'an 710049, China

(*Received* 30 *July* 1994 *and in final form* 30 *January* 1995)

1. INTRODUCTION

The natural circulation of closed-loop thermosyphons has stimulated a great deal of interest because of their wide applications, for example as solar heaters, and in cooling engines, turbine blades, computers, transformers and natural convection heat exchangers [1, 2]. The circulation is driven by thermally generated density gradients, which yield reliability, and low cost and noise-free advantages. There is a large volume of literature devoted to this subject as reviewed by Greif [3]. A more recent study for the natural circulation has been presented by Bernier and Baliga [4] in 1992. Here, only the relevant papers about 2D numerical calculations for such rectangular thermosyphons will be discussed briefly.

The traditional 1D model is insufficient when the flow inside the loop is significantly affected by buoyancy forces. Durig and Shadday [5] carried out a 2D numerical simulation of mixed-convection flow to improve the accuracy. The average friction factors and heat transfer coefficients have been calculated separately for the heated and cooled sections of a thermosyphon loop with vertical heat transfer sections. The 2D numerical simulation for the circulation in a thermosyphon loop with heating and cooling isolated in two vertical tubes joined together by isothermal upper and lower plenums was carried out by Lewis *et al.* [6] using parabolic equations. A new model has been proposed by Bernier and Baliga [4] with governing equations in elliptic forms, and its solving method involves an iterative procedure to couple the local results of 2D numerical simulation performed in the heated and cooled sections with those in a 1D analysis. The agreement between the predictions and the experimental results was good, but the predictive model was somewhat complicated. Meanwhile, the assumption of fanning friction factor $f = 16/Re$ may cause inaccuracy when the flow was strongly mixed-convective.

The present work will focus on a loop with a horizontal heated section, and the difference between the performance of a loop with vertical and horizontal heated sections will be discussed. In addition a comparison of the numerical results with the experimental data of Bernier and Baliga [4] will be made.

2. THEORETICAL ANALYSIS

The rectangular loops shown in Fig. 1 are heated over the bottom horizontal leg or over the lower half of the vertical left pipe and cooled over the upper part of the right pipe with the rest of the loop being thermally insulated. The flow is assumed to be in the axial direction which is only a function of the radius. The effect of curvature in a rectangular loop is negligibly small if the aspect ratio is large enough. The axial conduction and viscous dissipation are both neglected and the Boussinesq approximation is invoked. As to the conditions stipulated at the heated section, two situations are considered: (1) UWT—the heated section is isothermal; (2) UHF—the heated section is heated with uniform heat flux.

We have the momentum and energy equations as follows:

$$-\frac{\partial P}{\partial s}-\xi\rho g+\mu\left(\frac{\mathrm{d}^2V}{\mathrm{d}r^2}+\frac{1}{r}\frac{\mathrm{d}V}{\mathrm{d}r}\right)=0 \tag{1}$$

$$V\frac{\partial T}{\partial s}=a\left(\frac{\partial^2 T}{\partial r^2}+\frac{1}{r}\frac{\partial T}{\partial r}\right) \tag{2}$$

where $\xi = 1$ for the upflow, $\xi = -1$ for the downflow and $\xi = 0$ for the horizontal flow. The Boussinesq approximation is adopted, i.e.

$$\rho = \rho_c(1-\beta(T-T_c)).$$

Integration of equation (1) along the loop yields

$$\frac{\rho\beta g}{L}\left(\int_u T\,\mathrm{d}s-\int_d T\,\mathrm{d}s\right)+\mu\left(\frac{\mathrm{d}^2V}{\mathrm{d}r^2}+\frac{1}{r}\frac{\mathrm{d}V}{\mathrm{d}r}\right)=0.$$

The boundary conditions are

$$r=r_0,\quad V(r_0)=0,\quad r=0,\quad \left.\frac{\mathrm{d}V}{\mathrm{d}r}\right|_{r=0}=\left.\frac{\partial T}{\partial r}\right|_{r=0}=0,$$

$$T|_{r=r_0}=T_w\,(\text{UWT})\quad\text{or}\quad -\lambda\left.\frac{\partial T}{\partial r}\right|_{r=r_0}=q\,(\text{UHF})$$

for heated section.

$T|_{r=r_0}=T_c$ for cooled section and $(\partial T/\partial r)|_{r=r_0}=0$ for the connecting pipes. The following dimensionless parameters are defined

$$Ra^*=\frac{g\beta(T_w-T_c)D^3}{av}\frac{D}{L}\quad\theta=\frac{T-T_c}{T_w-T_c}$$

for UWT of heated section;

$$Ra^*=\frac{g\beta qD^4}{avk}\frac{D}{L}\quad\theta=\frac{T-T_c}{qr_0/k}$$

for UHF of heated section; and

$$W=\frac{VD^2}{Ra^{*1/2}aL}\quad x=\frac{s}{L}\quad\eta=\frac{r}{r_0}Ra^{*1/4}$$

† Author to whom correspondence should be addressed.

NOMENCLATURE

a	thermal diffusivity
c_p	specific heat of the fluid
D	internal diameter of the pipes, $2r_0$
f	Fanning friction factor
k	thermal conductivity
L	total length of the loop
Nu	Nusselt number
P	pressure
Pr	Prandtl number
q	heat flux
r	radial coordinate
r_0	internal radius of the pipe
Ra	Rayleigh number
Ra^*	modified Rayleigh number
Re	Reynolds number
s	axial coordinate along the loop
T	temperature of the fluid
V	axial velocity
W	dimensionless velocity
x	dimensionless axial coordinate.

Greek symbols

β	thermal expansion coefficient
η	dimensionless radial coordinate
θ	dimensionless temperature
μ	viscosity
ν	kinetic viscosity
ρ	density of the fluid.

Subscripts

b	bulk
c	cooled
d	downflow
h	heated
m	average
u	upflow
w	wall.

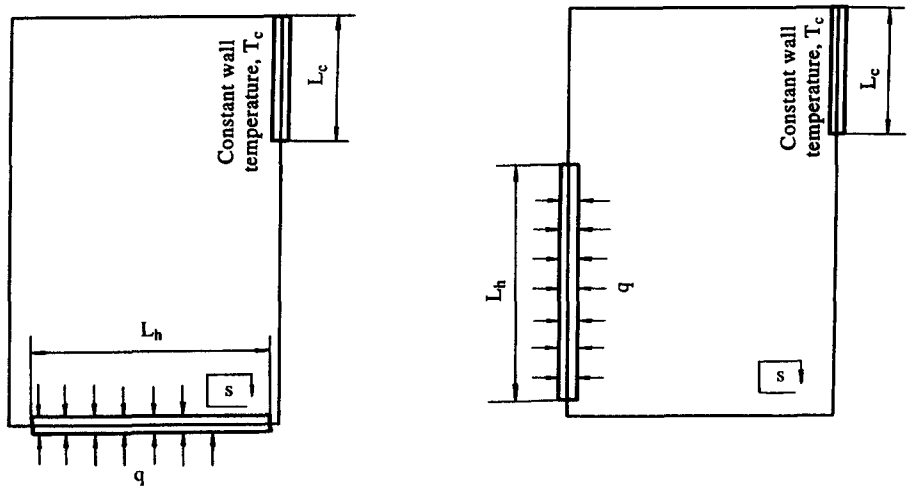

Fig. 1. Schematic illustration of a rectangular thermosyphon loop.

for both of the above cases. Then, the following dimensionless equations can be obtained

$$W\frac{\partial\theta}{\partial\eta} = 4\left(\frac{\partial^2\theta}{\partial\eta^2} + \frac{1}{\eta}\frac{\partial\theta}{\partial\eta}\right) \tag{3}$$

$$4\left(\frac{d^2W}{d\eta^2} + \frac{1}{\eta}\frac{dW}{d\eta}\right) + S_w = 0 \tag{4}$$

where S_w is the difference of the integration of θ along the upflow and that along the downflow, i.e.

$$S_w = \int_u \theta\,dx - \int_d \theta\,dx \tag{5}$$

with dimensionless boundary conditions

$$\eta = Ra^{*1/4} \quad W(Ra^{*1/4}) = 0$$

$$\eta = 0 \quad \left.\frac{dW}{d\eta}\right|_{\eta=0} = \left.\frac{\partial\theta}{\partial\eta}\right|_{\eta=0} = 0$$

$$\theta|_{\eta=Ra^{*1/4}} = 1 \quad \text{(UWT)}$$

or

$$\left.\frac{\partial\theta}{\partial\eta}\right|_{\eta=Ra^{*1/4}} = \frac{1}{Ra^{*1/4}} \quad \text{(UHF) for the heated section;}$$

$\theta|_{\eta=Ra^{*1/4}} = 0$ for the cooled section; and $(\partial\theta/\partial\eta)|_{\eta=Ra^{*1/4}} = 0$ for the connecting pipes.

The (fRe) and Nusselt number will be

$$fRe = -\frac{\mu\left.\frac{dV}{dr}\right|_{r=r_0}}{\frac{1}{2}\rho V_m^2} \tag{6}$$

or in dimensionless form

$$fRe = -4\frac{Ra^{*1/4}}{W_m}\left.\frac{dW}{d\eta}\right|_{\eta=Ra^{*1/4}} \tag{6'}$$

$$Nu(x) = -\frac{2Ra^{*1/4}}{(1-\theta_b)}\left.\frac{\partial\theta}{\partial\eta}\right|_{\eta=Ra^{*1/4}} \quad \text{(UWT)} \tag{7}$$

$$Nu(x) = \frac{2}{\theta_w - \theta_b} \quad \text{(UHF)} \tag{8}$$

for the heated section and

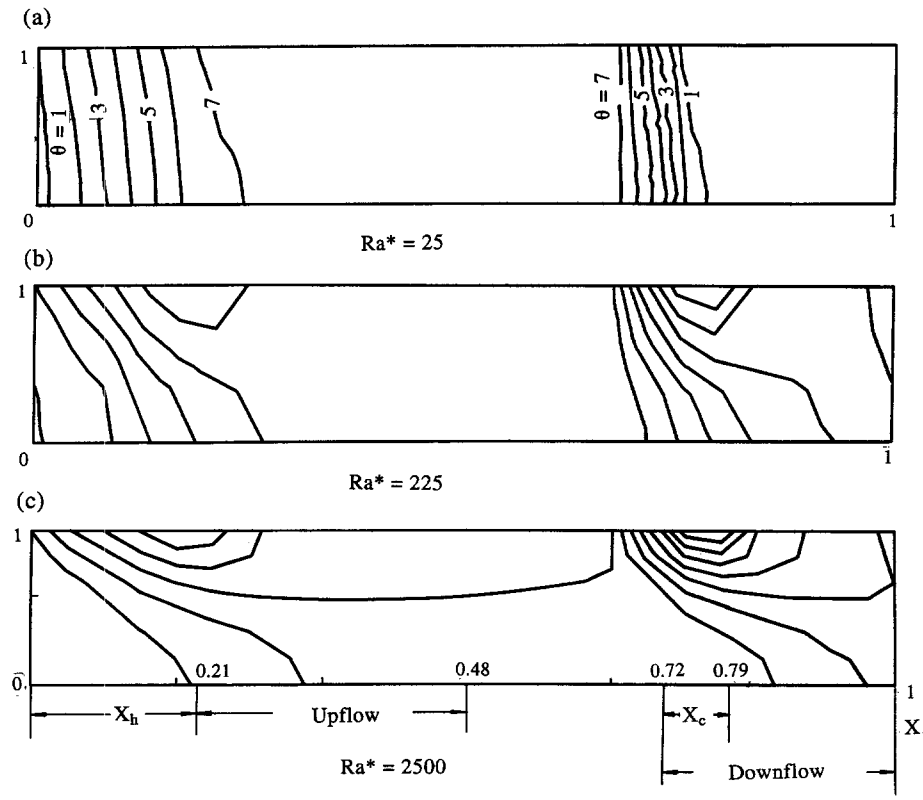

Fig. 2. Isotherm contours of the loop.

$$Nu(x) = -\frac{2Ra^{*1/4}}{\theta_b}\left.\frac{\partial\theta}{\partial\eta}\right|_{\eta=Ra^{*1/4}} \tag{9}$$

for the cooled section. The bulk temperature can be obtained from

$$\theta_b = \frac{\int_0^{Ra^{*1/4}} 2\pi\theta W\eta\,d\eta}{\int_0^{Ra^{*1/4}} 2\pi W\eta\,d\eta} = \frac{2}{W_m Ra^{*1/2}}\int_0^{Ra^{*1/4}} \theta W\eta\,d\eta. \tag{10}$$

Equations (3) and (4) are discretized by the finite-difference method, and are simultaneously solved with the TDMA (tri-diagonal matrix algorithm) method. It is noted that equation (3) is an initial problem along the streamwise direction. The initial values are corrected by the additional conditions that the inlet values should be equal to the outlet values. The numerical simulation is accomplished along the streamwise direction step by step. The operations are repeated until convergence is obtained, which is assessed in terms of the invariance of each field of the two succesive calculations, i.e. the absolute value of the difference between the variables for the two successive calculations divided by the absolute value of the last iteration is less than 10^{-5}.

A series of grid sensitivity runs were performed which suggested that satisfactory results could be obtained using 30×40 mesh for the lower Ra^* and 30×50 for the higher Ra^*.

3. RESULTS AND DISCUSSIONS

The performance of a rectangular thermosyphon loop with vertical or horizontal heat transfer section has been studied. Except for the different location of the heated section, all other conditions remain unchanged as in Fig. 1. Values of $x_h = 0.256$ and $x_c = 0.074$ are chosen as the dimensionless lengths of heated and cooled sections in the presentation of the results. For the sake of conciseness and because of the close similarities of UWT and UHF for the heated section, only the results of UHF will be presented here.

The isotherm contours and velocity profiles are shown to change with Ra^* (see Figs. 2 and 3). At low Ra^*, the stratified temperature distribution in Fig. 2(a) reveals the importance of the axial conduction. With the increase in Ra^*, the isotherm contours begin to deflect suggesting the development

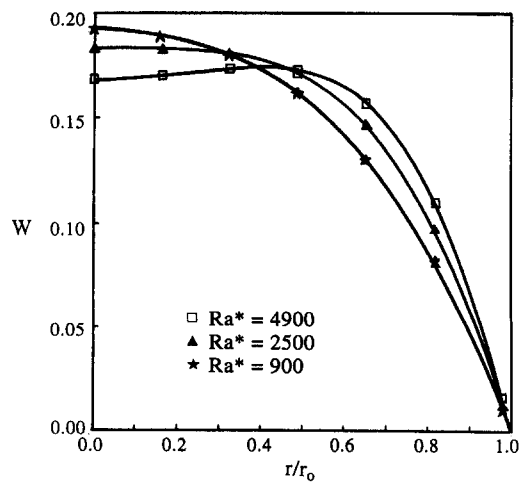

Fig. 3. Velocity profiles as a function of Ra^*.

and intensification of the convection. For the experiment reported in ref. [4], in which the values of Ra^* range from 3110 to 17 880, the convective effects might be large enough to overshadow the effect of axial conduction so that the axial conduction could be neglected.

Figure 3 reveals that the velocity profile is distorted from a parabolic shape under high Ra^*, which indicates that the buoyancy forces play an important role. Such distortion is especially pronounced for the closed loop with vertical heated sections (Fig. 4), because the fluid nearby the heated wall will be subjected to strong buoyancy forces in the streamwise direction. While for the horizontally heated loop, the buoyancy forces act in the transverse direction of the mainstream, the effect will be unnoticeable at low Ra^*. This is in accordance with the conclusion drawn from the 1D model [7]. It is noted that $f\,Re = 16$ is true only for very low Ra^* as shown in Fig. 5.

It is of interest to transform the dimensionless velocity as

$$W = \frac{1}{Ra^{*1/2}/Re\,Pr\dfrac{D}{L}} = \frac{Pr^{1/3}\left(\dfrac{D}{L}\right)^{1/2}}{(Ra^{1/4}/Re^{1/2}Pr^{1/3})^2}. \quad (11)$$

For the same Pr and D/L, as Ra^* increased, the value of $(Ra^{1/4}/Re^{1/2}Pr^{1/3})$ becomes larger under smaller W_m for the vertically heated loop, thus indicating a larger proportion of natural convection in the flow, in accord with ref. [8]. When Ra^* is small, $(Ra^{1/4}/Re^{1/2}Pr^{1/3})$ is nearly the same for both vertical and horizontal cases as shown in Fig. 4.

Figure 6 shows the comparison of the cooled section Nusselt numbers between the vertically heated loop and the horizontally heated loop. The difference of Nu for the heated section is even smaller. It is noted that the predicted difference of Nusselt numbers between the two cases could be negligible even at sufficiently high Ra^*. In fact, the mixed-convection flow is beneficial in enhancing heat transfer. It can be seen from equation (4) that the temperature difference of the upflow and downflow is the only motivation of the circulation, i.e. the present assumption of the axial flow considers the streamwise buoyancy forces only, which fails to take account of the transverse mixed-convection for the horizontal heated section, so a higher heat transfer rate can be expected if elliptic governing equations are adopted. Nevertheless, the present model will not mask the important physical processes associated with this problem. The present numerical results agree well with the experimental data in ref. [4] (Table 1 and Fig. 7).

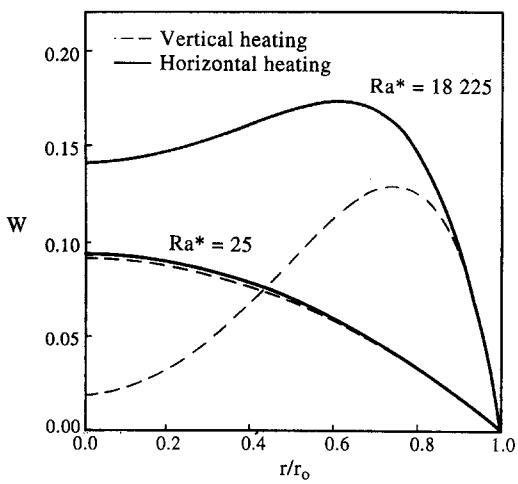

Fig. 4. Comparison of velocity profiles.

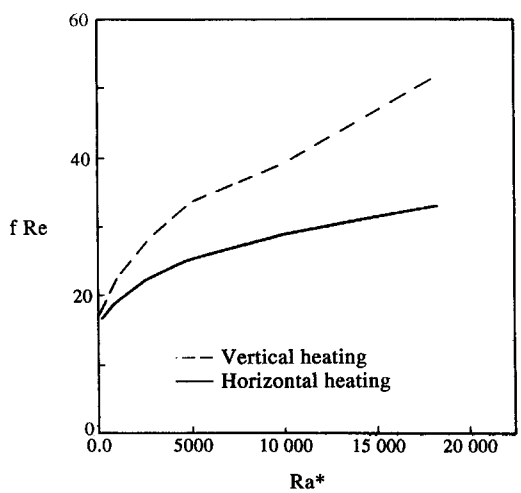

Fig. 5. $f\,Re$ as a function of Ra^*.

4. CONCLUDING REMARKS

A 2D model has been proposed to calculate the entire rectangular thermosyphon loop with either a vertical or horizontal heat transfer section. With this model, we have presented the temperature and velocity profiles vs Ra^* and investigated the difference existing in the loops with vertical or

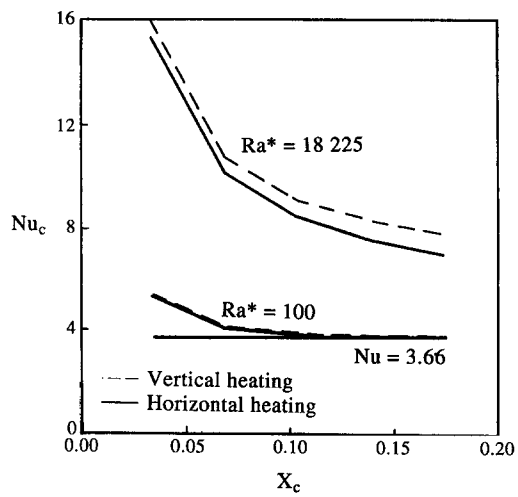

Fig. 6. Nu of cooled section.

Table 1. Comparison of V_s (cm s^{-1}) between numerical results and experimental data

Experiment [4]	Present model	Prediction in [4]
0.457	0.484	0.465
0.483	0.489	0.473
0.628	0.622	0.626
0.722	0.800	0.704
0.679	0.720	0.690
0.776	0.808	0.756
0.739	0.780	0.746
0.845	0.867	0.814

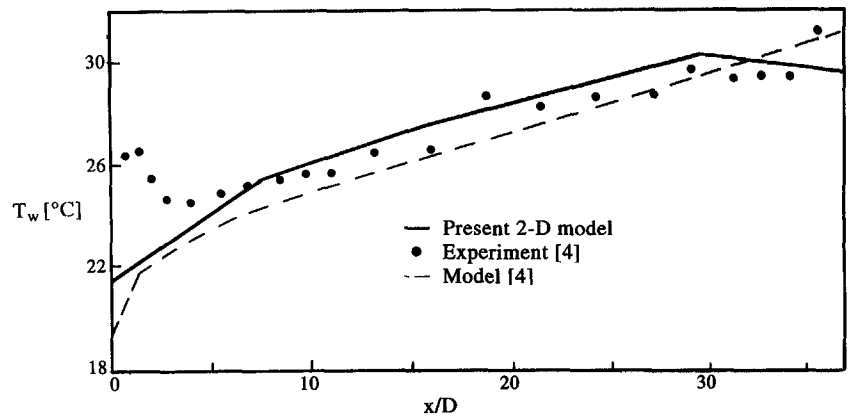

Fig. 7. Comparison of T_w between numerical results and experimental values.

horizontal heat transfer section. It is shown that the distortion of the velocity profile for the vertically heated loop is more noticeable under high Ra^*, and the friction factor increases with Ra^* at a larger rate than for the horizontally heated loop, while the difference in Nusselt numbers is small.

REFERENCES

1. D. Japkise, Advances in thermosyphon technology. In *Advances in Heat Transfer* (Edited by T. F. Irvine and J. P. Hartnett), Vol. 9, pp. 1–111. Academic Press, New York (1973).
2. M. G. Parent, Th. H. Van Der Meer and K. G. T. Hollands, Natural convection heat exchangers in solar water heating systems: theory and experiment, *Solar Energy* **45,** 43–52 (1990).
3. R. Greif, Natural circulation loops, *ASME J. Heat Transfer* **110,** 1243–1258 (1988).
4. M. A. Bernier and B. R. Baliga, A 1-D/2-D model and experimental results for a closed-loop thermosyphon with vertical heat transfer sections, *Int. J. Heat Mass Transfer* **35,** 2969–2982 (1992).
5. B. R. Durig and M. A. Shadday, Flow in a rectangular closed-loop thermosyphon with vertical heat transfer passages, ASME paper 86-WA/HT-78 (1986).
6. J. S. Lewis, M. W. Collins and P. H. G. Allen, Flow rate prediction for a thermosyphon loop, *Proc. of the 9th Int. Heat Transfer Conf.*, Jerusalem, Israel, Vol. 2, pp. 549–554 (1990).
7. B. J. Huang and R. Zelaya, Heat transfer behavior of a rectangular thermosyphon loop, *ASME J. Heat Transfer* **110,** 487–493 (1988).
8. J. R. Lloyd and E. M. Sparrow, Combined forced and free convection on vertical surfaces, *Int. J. Heat Mass Transfer* **13,** 434–438 (1970).